Synthesis, Characterisation and 3D Printing of an Isosorbide Based, Light Curable, Degradable Polymer for Potential Application in Maxillofacial Reconstruction

N. Owji[1, 5], A. Aldaadaa[1, 3], J-R. Cha[4], T. Shakouri, E. García-Gareta[5], H-W. Kim[4], J. C. Knowles[1, 2, 5*]

[1]Division of Biomaterials and Tissue Engineering, Eastman Dental Institute, University College London, 256 Gray's Inn Road, London WC1X 8LD, UK

[2]The Discoveries Centre for Regenerative and Precision Medicine, UCL Campus, London, UK

[3]Division of Maxillofacial Diagnostic, Medicine & Surgical Sciences, Eastman Dental Institute, University College London, 256 Gray's Inn Road, London WC1X 8LD, UK

[4]Institute of Tissue Regeneration Engineering (ITREN), Dankook University, Cheonan 330-714, Republic of Korea

[5]RAFT, Regenerative Biomaterials Group, The RAFT Institute, Mount Vernon Hospital, Northwood, UK

Corresponding Author's Email: j.knowles@ucl.ac.uk

KEYWORDS

Bone Tissue Engineering, Polymer Synthesis, 3D Printing, Maxillofacial Reconstruction

ABSTRACT

Although emergence of bone tissue engineering techniques has revolutionised the field of maxillofacial reconstruction, the successful translation of such products, especially concerning larger sized defects, still remains a significant challenge.

Light curable methacrylate-based polymers have ideal properties for bone repair. These materials are also suitable for 3D printing which can be applicable for restoration of both function and aesthetics. The main objective of this research was to synthesise a mechanically stable and biologically functional polymer for reconstruction of complex craniofacial defects. The experimental work initially involved synthesis of (((3R,3aR,6S,6aR)-hexahydrofuro[3,2-b]furan-3,6-diyl)bis(oxy))bis(ethane-2,1-diyl) bis((4-methyl-3-oxopent-4-en-1-yl)carbamate), CSMA-1, and ((((((((((((3*R*,3a*R*,6*S*,6a*R*)-hexahydrofuro[3,2-*b*]furan-3,6-diyl)bis(oxy))bis(ethane-2,1 diyl))bis(oxy))bis(carbonyl))bis(azanediyl))bis(methylene))bis(3,3,5-trimethylcyclohexane-5,1-diyl))bis(azanediyl))bis(carbonyl))bis(oxy))bis(ethane-2,1-diyl) bis(2-methylacrylate), CSMA-2; Nuclear Magnetic Resonance (NMR) analysis confirmed formation of the monomers and composite samples were fabricated respectively by exposing 11 mm diameter discs to blue light. Modulus of the tensile elasticity was tested using a biaxial flexural test and the values were found to be between 1 and 3 GPa in CMA-1, CSMA-2 and their composites. *In vitro* cell culture, using human Bone Marrow Derived Mesenchymal Stem Cells (BMSCs), confirmed non-toxicity of the samples and finally 3D printing allowed direct photo-polymerisation and setting of the bio ink into a mesh-like construct.

INTRODUCTION

Trauma, congenital defects and oncological tissue resection are the major cause of bone loss in the human body (1). Based on data from the Journal of Oral and Maxillofacial Surgery (2), approximately 7% (227500) of the new born children in the United Kingdom are affected by genetic abnormalities of the head and face every year . Traditionally most traumatic incidents were caused by automobile accidents. However, more recently, 60% of severe facial injuries are a result of assaults, domestic violence and falls (3). Furthermore, Cancer Research UK has reported 12061 cases of head and neck cancers in 2015 with a survival rate of 19%-59% (4). Such unfortunate events have raised the demand for a suitable material to restore bone defects in the oral and craniofacial region.

There has been a significant change towards the repair approach over time based on the defect size and the material of choice. Emergence of autologous bone grafts since 1978 has revolutionised the field of maxillofacial reconstruction (5). Although this is still considered as the gold standard technique due to excellent osseointegration and osteogenesis, downsides of the harvesting procedure, postoperative pain, infection and the risk of graft failure argue in favour of alternative techniques (6). The use of alloplastic bone substitutes offers short operative time, lower cost and elimination of donor site morbidity. However, poor aesthetic outcomes, chronic pain syndrome especially in oncologic patients and poor long-term results are the major disadvantages associated with these implants (7).

Tissue engineering is an interdisciplinary field that combines material science, principles of engineering and biology to restore, replace or improve biological function (8).

Polymeric based scaffolds in the field of tissue engineering are divided into synthetic and naturally occurring. Collagen, gelatin and hyaluronic acid are natural polymers that have been approved by the FDA; however, unpredictability of the degradation kinetics and poor mechanical properties has led to emergence of synthetic polymers that are biocompatible and biodegradable (9). For new bone formation, a successful combination of osteoconduction, osteogenesis and osteoinduction is critical. Therefore, synthetic scaffolds need to incorporate such features to allow restoration of bone defects (10).

Poly (glycolic acid) (PGA), polylactic acid (PLA) and copolymer (PLGA) are widely used in the clinical environment. However, when large PLGA prosthetics are implanted, a decrease in molecular weight and loss of strength will lead to bulk degradation, releasing high levels of lactic acid and glycolic acid resulting in pH drop and eventually tissue loss(11). Poly (ε-caprolactone) (PCL) has also been extensively investigated for use in craniofacial reconstruction, however, PCL is slow to degrade (12) and when implanted often exhibits inadequate cell attachment and insufficient tissue integration due to its hydrophobic nature (13). Similarly, structures made from composite materials such as polyamide/hydroxyapatite are being explored but with limited success due to poor mechanical stiffness(14).

Various proteins may be used to stimulate osteogenesis and neovascularization. Bone Morphogenic Protein (BMP) is part of the transforming growth factor and has been successfully used to promote new bone growth (15). Vascular Endothelial Growth Factor (VEGF) has been used in conjunction with BMPs to enhance bone formation by stimulating angiogenesis (16). However, delivery of BMPs requires molecular carriers and their mechanical properties are not biomimetic of the native bone (17), moreover cost remains a limiting factor regarding its use in clinical settings.

PCL diacylate (PCLDA)(18), and PEG diacylate (PEGDA) (19), which are biodegradable, photo curable polymers have brought forth new options toward the fabrication of biomedical devices and scaffolds. Photo curable polymeric materials are suitable for bone tissue engineering with high Young's modulus and reduced degradation rate [(20), (21)]. In previous studies, the synthesis and properties of isosorbide based dimethacrylic monomer with potential for dental and bone tissue repair applications have been investigated [(22), (23)].

In this research we have developed a light curable degradable polymer, targeted at reconstruction of maxillofacial defects, which also has the potential to be used in 3D printing. Both CSMA-1 and CSMA-2 were synthesised using bis(2-hydroxyethyl) isosorbide (BHIS) as a starting material. The reaction utilises a simple K_2CO_3 catalyst which is easily removed. Finally, mechanical properties of the polymers can be controlled by incorporation of a solvent such as triethylene glycol dimethacrylate (TEGDMA), at different ratios to CSMA-1 and CSMA-2.

MATERIALS

1,4:3,6-dianhydro-D-sorbitol (isosorbide, 98%), ethylene carbonate (99%), dibutyltin dilaurate (DBTDL, 95%), 2-isocyanatoethyl methacrylate (IEM, 98%), isophorone diisocyanate (IPDI, 98%), and 2-hydroxyethyl methacrylate (HEMA, 97%) were obtained from Sigma-Aldrich (St Louis, MO, USA).

Commercial acrylate monomer triethylene glycol dimethacrylate (TEGDMA, 95%) and UV photoinitiators (PI) phenylbis (2,4,6-trimethylbenzoyl) phosphine oxide (BAPO) were obtained from Sigma-Aldrich (St Louis, MO, USA).

Potassium carbonate (99.5%), ethyl acetate (99.5%), *n*-hexane (99.5%), methanol (99.5%), and chloroform (99.5%) were supplied by Daejung Chem. Co. Ltd. (Seoul, Korea).

EXPERIMENTAL METHODS

CSMA-1 synthesis

1st step: preparation of bis(2-hydroxyethyl) isosorbide (BHIS)

The intermediate chemical compound, BHIS, was synthesised using isosorbide and ethylene carbonate. A mixture of isosorbide (684.3 mmol) and ethylene carbonate (1,505.5 mmol) in a 500 mL of two-necked round bottom flask was degassed with nitrogen for 1 hour. The reaction mixture was then heated in nitrogen at 70 °C for 1 hour. After the solid contents were melted completely, K_2CO_3 (68.4 mmol) was added to the reaction mixture and reacted at 170 °C for 48 hours. The synthesised BHIS was purified by silica column chromatography using methanol/ethyl acetate (1/9) and dried at 60 °C for 24 hours under vacuum to obtain high purity BHIS (**Scheme 1**).

2nd step: preparation of (((3R,3aR,6S,6aR)-hexahydrofuro[3,2-b] furan-3,6-diyl)bis(oxy))bis(ethane-2,1-diyl) bis((4-methyl-3-oxopent-4-en-1-yl)carbamate)

A mixture of BHIS (246.9 mmol) and IEM (518.5 mmol) was dissolved in 200 mL of chloroform and stirred under a dry nitrogen atmosphere (99.9%) at 25 °C for 1 hour. 8 drops

of DBTDL were slowly added into the mixture. This mixture was continuously stirred at 25 °C for 12 hours and then evaporated in *vacuo* to give the crude product. Finally, the synthesised CSMA was purified by column chromatography using hexane/ethyl acetate (1/2) and dried at 60 °C for 24 hours under vacuum to obtain a viscous sticky colourless fluid.

CSMA-2 synthesis

CSMA - 2 was prepared by a two-step reaction from BHIS, and IPDI, followed by a reaction between the NCO-terminated monomer and HEMA. The BHIS (246.9 mmol) and IPDI (518.5 mmol) were dissolved in chloroform (200 mL). The reaction mixture was stirred under nitrogen at 25°C for 1 h. 8 drops of DBTDL were slowly added into the reaction mixture. The reaction mixture was continuously stirred for at 25 °C for 12 hours. HEMA (518.5 mmol) was added into the reaction mixture. The reaction mixture was continuously stirred for at 25 °C for 12 hours and then evaporated in *vacuo* to give the crude product. Finally, the synthesised CSMA was purified by column chromatography using hexane/ethyl acetate (1/2) and dried at 60 °C for 24 hours under vacuum to obtain a white powder. (**Scheme 2**).

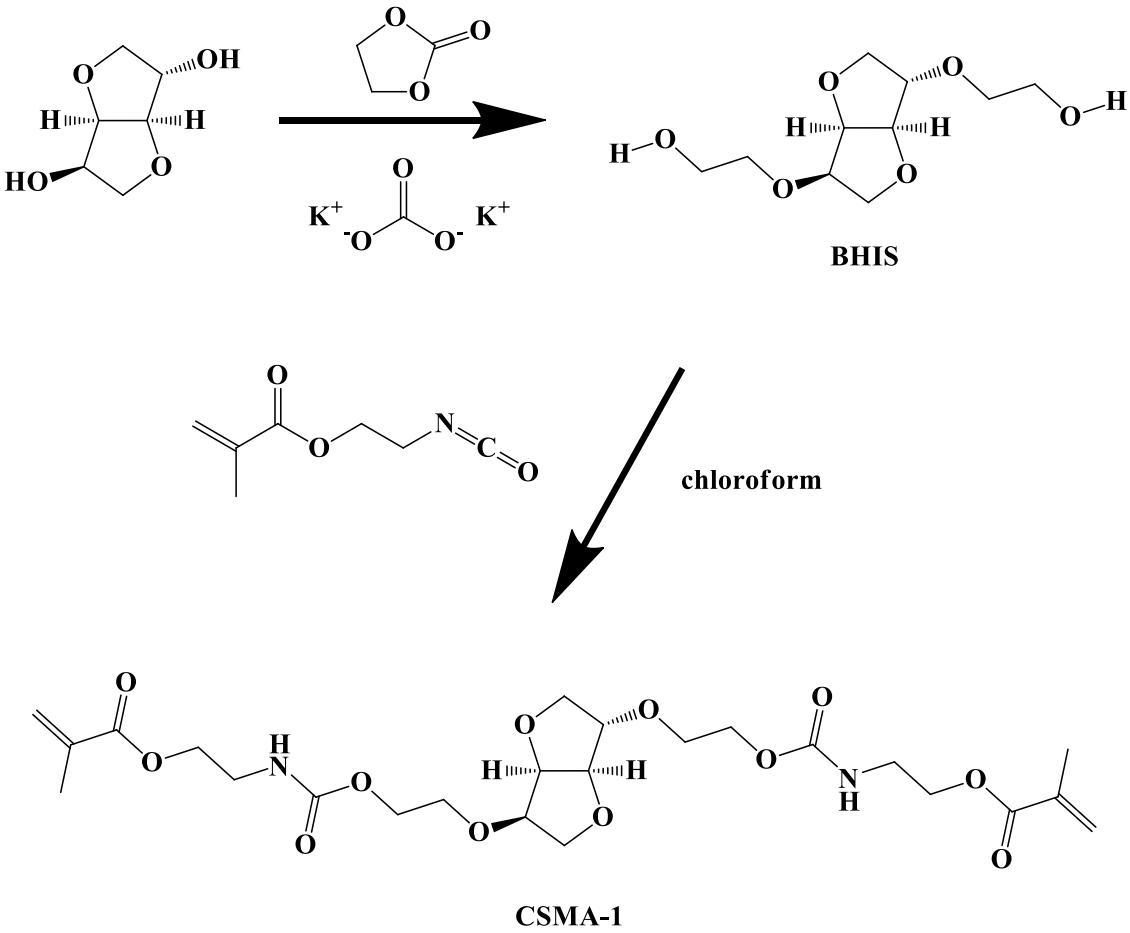

Scheme 1. Preparation of (((3R,3aR,6S,6aR)-hexahydrofuro[3,2-b]furan-3,6-diyl)bis(oxy))bis(ethane-2,1-diyl) bis((4-methyl-3-oxopent-4-en-1-yl)carbamate)

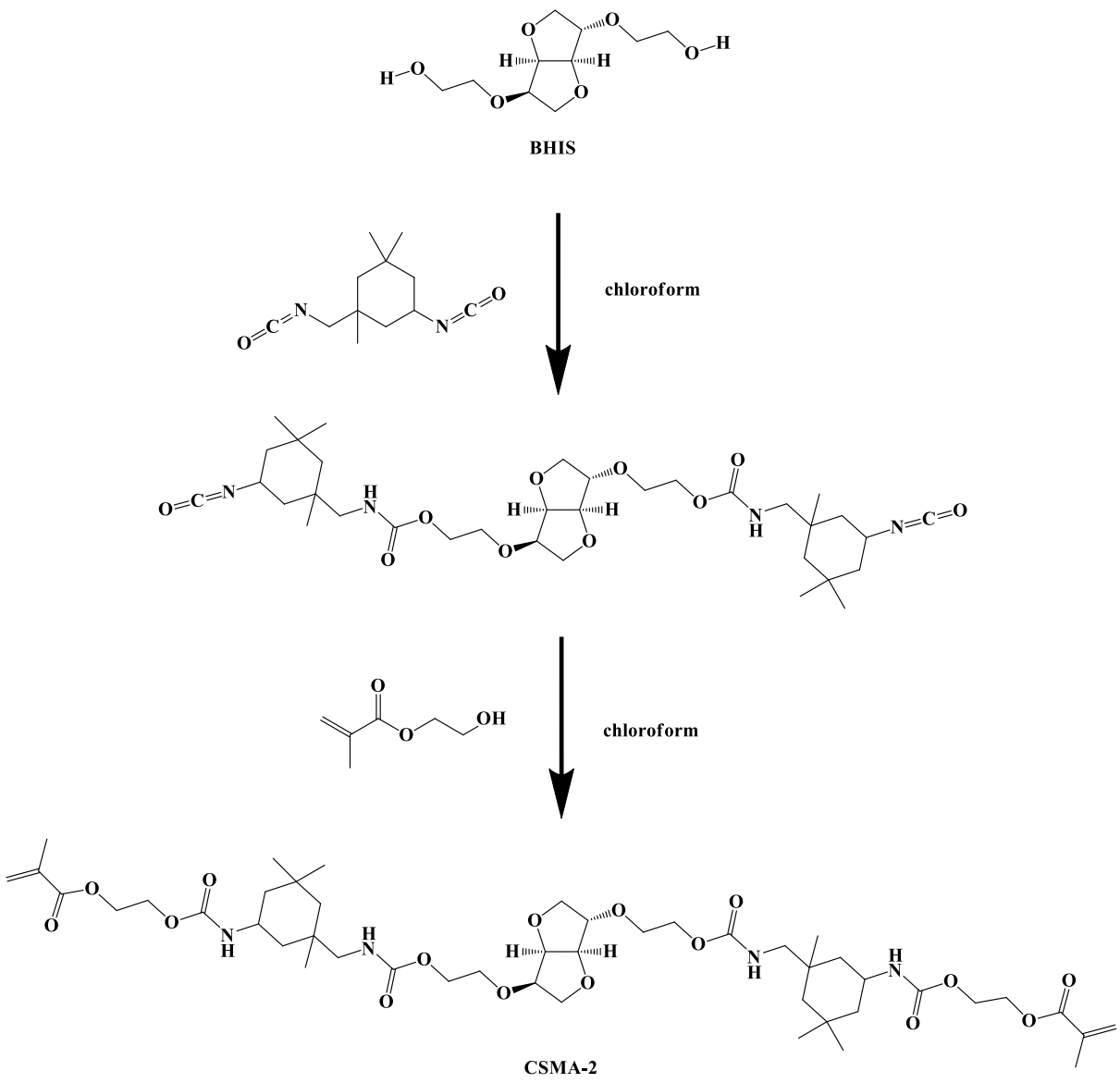

Scheme 2. Preparation of ((((((((((3R,3aR,6S,6aR)-hexahydrofuro[3,2-b]furan-3,6-diyl)bis(oxy))bis(ethane-2,1-diyl))bis(oxy))bis(carbonyl))bis(azanediyl))bis(3,3,5-trimethylcyclohexane-5,1-diyl))bis(azanediyl))bis(carbonyl))bis(oxy))bis(ethane-2,1-diyl) bis(2-methylacrylate)

Nuclear Magnetic Resonance (NMR) and Gas Chromatography (GC)

The ^{1}H NMR spectra were recorded with AVANCE III 600 spectrometer (600 MHz, Bruker, Germany) spectrometer and $CDCl_3$ as a solvent. All data were given as chemical shifts (δ, ppm) downfield from tetramethylsilane.

Gas chromatography high resolution mass spectra (GC-MASS) were recorded on a JEOL JMS-700 (JEOL, Japan) spectrometer in Fast Atom Bombardment (FAB) mode.

Degree of conversion

Fourier Transform Infrared Spectroscopy (FTIR, System 2000, PerkinElmer, Seer Green, UK) was used in order to determine the rate of monomer conversion. The polymer paste was placed on the diamond of an attenuated total reflectance accessory (Golden Gate ATR, Specac Ltd., Orpington, UK), and upon exposure to blue light spectra were recorded for 1200 s.

Composite preparation

In order to prepare the Calcium Phosphate (CaP) incorporated composite paste, CSMA-1 and CSMA-2 monomers were initially mixed with 1 wt % camphorquinone (CQ, DMG) photo initiator. A mixture of Mono-Calcium Phosphate Monohydrate (MCPM) and Beta Tri-Calcium Phosphate (TCP) was subsequently mixed with the monomers at various concentrations, using a centrifugal planetary mixer (SpeedMixer, Hauschild Engineering, Hamm, Germany) at 1700 rpm for 2 min. The specimens were then moulded by applying the mixture of composites into 11 mm diameter disc shaped metal circlips. Finally, to allow photo

polymerisation, blue light with a wavelength of 450-470 nm was applied to the specimens for 40 seconds (which was calculated based on the degree of monomer conversion).

Mechanical properties

The mechanical properties of the composite discs were examined by performing a Biaxial Flexural Strength (BFS) test. This involved applying a load via a 2 kN load cell and ball-on-ring jig at a speed of 1 mm/min using a Shimadzu Autograph AGS-X, (Shimadzu, Milton Keynes, UK) on the discs until the specimens failed.

Percentage mass change

The specimens were immersed in water and the weight was measured by using a balance accurate to 4 places (OHAUS, US) at various time intervals to compare the final dry mass with the initial time point. This was carried out by air drying the discs in all the time points followed by using a vacuum oven at the last time interval (7 months post immersion in water).

pH values

The samples were immersed in 10 ml of Dulbecco's modified Eagle's medium (Gibco®, Life Technologies Ltd., Paisley, UK) and placed in a CO_2 incubator. The pH values were measured by using a pH meter (Orion star A111Thermo Scientific, UK). The pH electrode was calibrated by using standard solutions of pH 4 and 7 prior to taking the measurements.

Biocompatibility studies

-Cell culture

Human BMSCs (Institute of regenerative medicine at the Texas A&M Health Science Centre College of Medicine (USA)) were cultured in polystyrene flasks in minimum essential medium (α-MEM, Gibco BRL) supplemented with 10% foetal bovine serum (FBS) (Invitrogen) and 100 U/ml of penicillin/streptomycin (P/S) (Sigma-Aldrich). Subsequently they were incubated at 37 °C at 5% CO2 and harvested for experiments once they reached 80% confluence at passage 4.

-Metabolic activity

Specimen discs were sterilised under UV light (254 nm) for 30 min and were then placed in 24 well tissue culture plates (Thermo Fisher Scientific, Loughborough, UK). 10000 cells per disc were seeded on each well and incubated at 37 °C 5% CO2. To determine cell proliferation, at day 1, 4 and 7 of culture, $0.1x10^{-3}$ L of alamar blue dye (alamar blue, ABD Serotrec) was added to each well and incubated for a further 4-h period. Fluorescence measurements (excitation wavelength of 530 nm and emission wavelength of 590 nm) were then taken using a Fluroscan Ascent plate reader (Labsystems, Helsinki, Finland). The ratio of fluorescence intensity of the reduced alamar blue compared with the control (Thermanox plastic coverslips, Thermo Fisher Scientific, UK) allowed calculation of relative cell viability.

Scanning Electron Microscopy (SEM) Images

Specimens were fixed in 3% glutaraldehyde and 0.1M cacodylate buffer and stored at 4˚C overnight. Serial ethyl alcohol dehydration was carried out the next day for 10 min at each concentration and the discs were subsequently dried in hexamethyldisilazane and left in the hood for 1 hour. Specimens were then coated with 95% gold and 5% palladium (Polaron E5000 Sputter Coater, Quoram Technologies, Laughton, UK) and SEM (Philips XL30 Field Emission SEM, Amsterdam, Netherlands) was used to visualise the surface of the specimen discs.

3D printing

The synthesised CSMA-2 was mixed 1 wt % CQ photo initiator. Digital Light Processing (DLP) technique was subsequently used to allow curing of the photopolymer resin using a DLP 3D printer (Nebel Superfine, XYZprinting, Taiwan). Initially the base setup was fixed at 8 base layers with a curing time of 19000 ms and the power intensity was set at 60 W/m^2. The model setup for curing was 10000 ms with power intensity of 53 W/m^2. Power level was arranged at 15% with waiting time of 0 ms for both base and model setups. Finally peeling speed of 0.2500 mm/s and distance of 5 mm were applied.

Statistical analysis

The results were statistically analysed using one-way analysis of variance (ANOVA) with Tukey's post hoc test; $p < 0.05$ was considered to be statistically significant.

RESULTS AND DISCUSSION

The two monomers developed in this work have methacrylate units that are linked to isosorbide through urethane linkage. CSMA-1 and CSMA-2 were prepared by the urethane coupling reaction between isocyanate group and hydroxyl group. CSMA-1 and CSMA-2 were then purified by column chromatography and used for material characterisation and 3D printing.

^{1}H NMR (**Fig.3**) and GC-MASS (**Fig.4**) analysis confirmed formation of monomers (CSMA-1 and CSMA-2) fabricated from isosorbide. ^{1}H NMR spectrum of BHIS, CSMA-1, and CSMA-2 showed the expected chemical shifts. ^{1}H NMR spectrum of synthesised BHIS is confirmed by the formation of ethylene group with signal of proton H_2-C-C-H_2 at 3.58~3.73 ppm. The three singlets showed at 6.12, 5.60, 1.95 ppm of CSMA-1 and 6.14, 5.59, and 1.96 ppm of CSMA-2 corresponded to the protons of the methacryl group (CH_2=C-CH_3). The signals between 2.92 and 0.91 ppm corresponded to the protons of the isophorone cycle. The protons of the urethane groups were not perceived at all, which could be due to being superimposed on other signals.

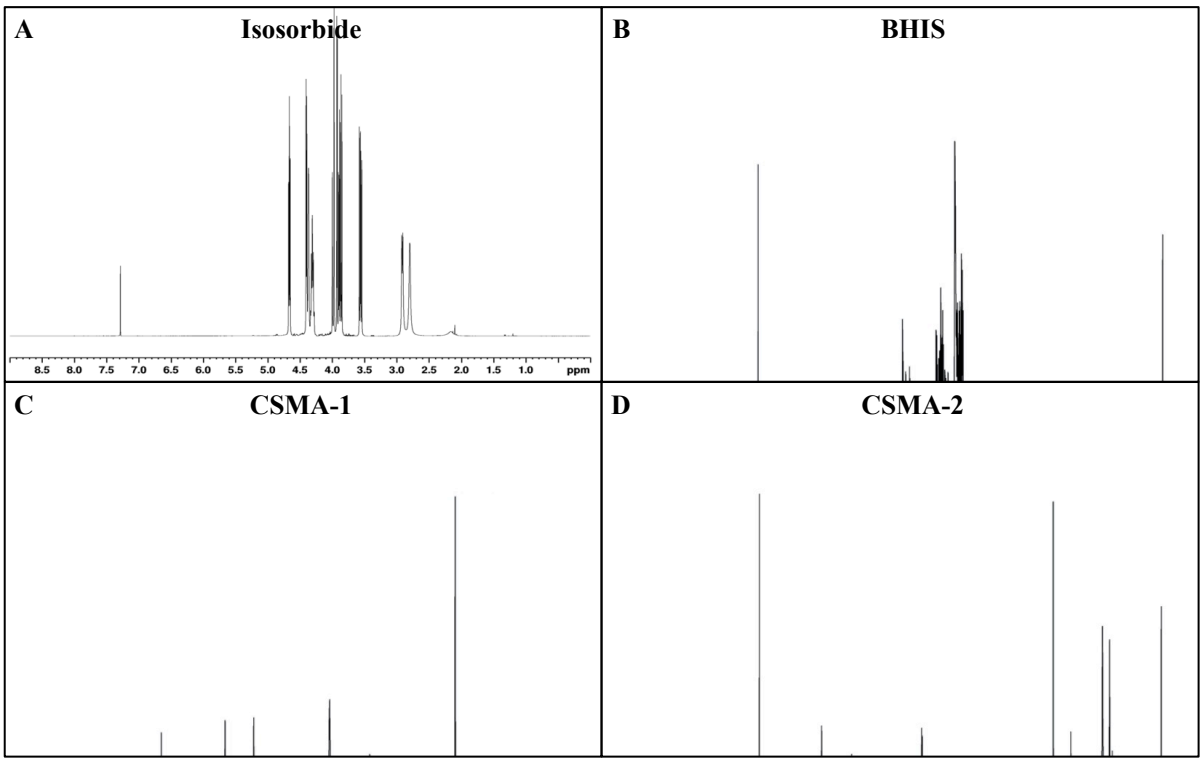

Fig.3. ^{1}H NMR spectra showing the presence of chemical bonds formation of isosorbide (A), BHIS (B) and the final CSMA-1(C) and CSMA-2 (D) monomers.

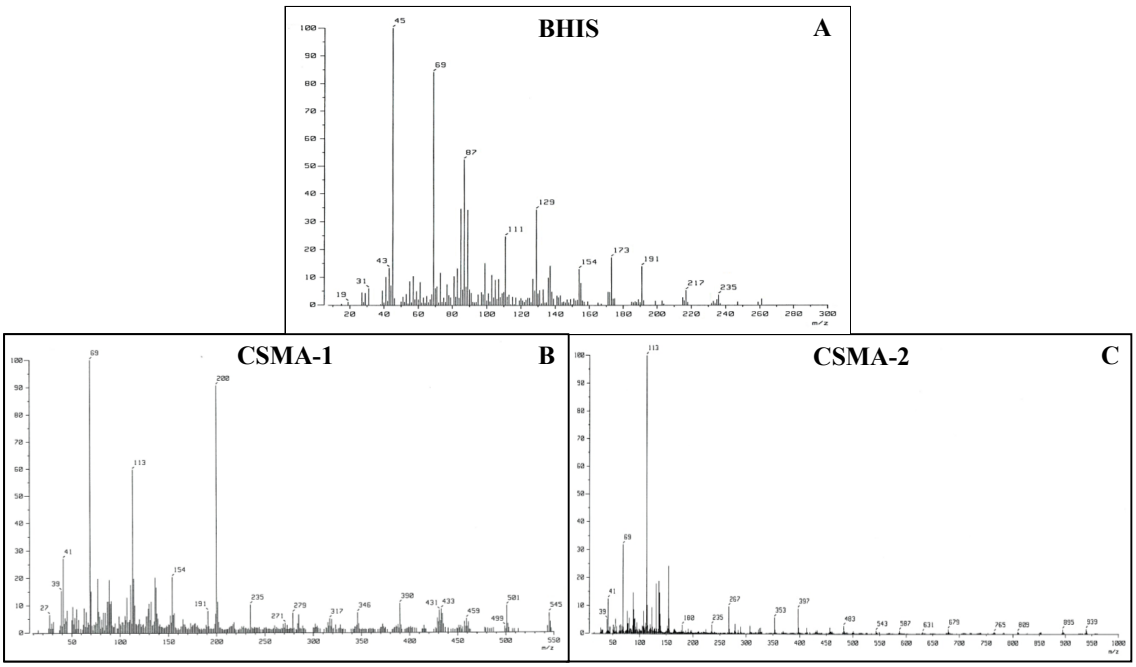

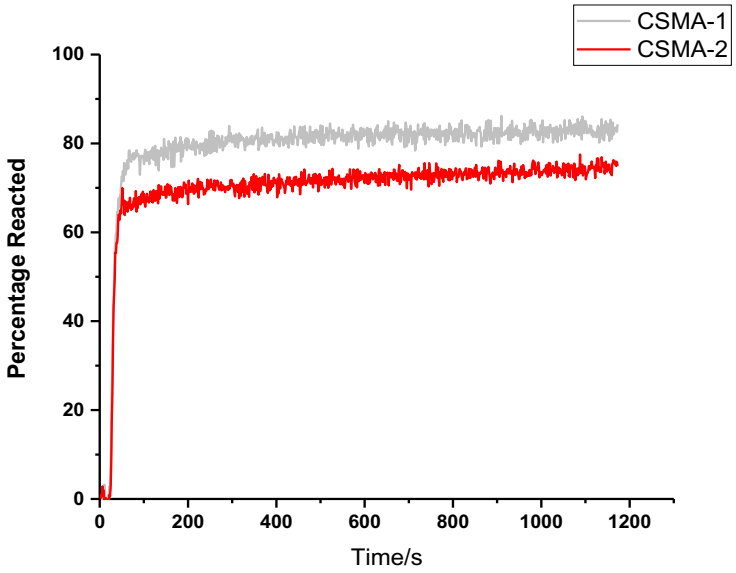

Fig. 4. GC-MASS spectra of BHIS (A), CSMA-1 (B), and CSMA-2 (C) followed by the FTIR spectra of CSMA-1 and CSMA-2 showing the rate monomer conversion post exposure to blue light in 1200 s.

The mass spectra of BHIS, CSMA-1, and CSMA-2 were observed at m/z 235, 545, and 939, respectively, and were matched to molecular ion of BHIS, CSMA-1, and CSMA-2. In CSMA-1 and CSMA-2, mass fragment peaks were observed corresponding to m/z 69, and 113, where methacrylate and ethyl methacrylate groups were present.

In order to calculate the optimum curing time upon photo polymerisation of the liquid phase,

Absorbance profiles were received at $1319 \pm 1\ cm^{-1}$ (C–O stretch bond) and $1334 \pm 2\ cm^{-1}$ (baseline) and used to calculate conversion using the following equation

$$C = \left[1 - \left(\frac{At}{A0}\right)\right] x\ 100$$

where C is conversion. A_f and A_0 are final and initial absorbance above baseline, respectively.

Over 60% conversion of both monomers were observed within the first 40 s, which suggested the curing time in composite preparation.

Mechanical stability is a key factor in determining the potential clinical implementation of a novel material in bone tissue engineering. In this study, initial comparison between the stiffness of CSMA-1 and CSMA-2 indicated higher values in CSMA-2; even though elastic modulus of the bone in non-load bearing regions is within the range of 0.1-0.5 GPa (24), significant drop in the values is expected to take place when implanted *in vivo* (25). Therefore, the focus of this research remained on the evaluation of CSMA-2 properties and the application of CSMA-1 can be dedicated to smaller sized defects in the craniofacial region.

Briefly, incorporation of two filler ratios was investigated in CSMA-1 (**Fig.5**); lower viscosity of this monomer allowed incorporation of 60 and 70% CaP, whereas 40 and 50% fillers were added to CSMA-2. The biaxial flexural modulus of the discs was predicted to show a linear

relationship with the filler content(26), where CaP ceramics increases the stiffness value. As expected, addition of higher amount of powder, 60% and 70% respectively, significantly improved the modulus compared to the polymer disc (**Fig.5**). This trend was not observed in CSMA-2 which could potentially be due to different rheological behaviour of this polymer compared to CSMA-1 (27); highly viscous nature of CSMA-2 as a function of shear rate exhibits a higher resistance to flow, this plays a major role in powder dispersion, and eventually forms a stiffer composite. Though it is crucial to consider having a higher friction can only allow certain amount of mixing upon powder addition. Therefore, the optimum formulation was found to be 50% CaP and it did not show any significant

difference in comparison with CSMA-2 polymer discs; this suggests an ideal dispersion of this filler formulation in the monomer phase(28).

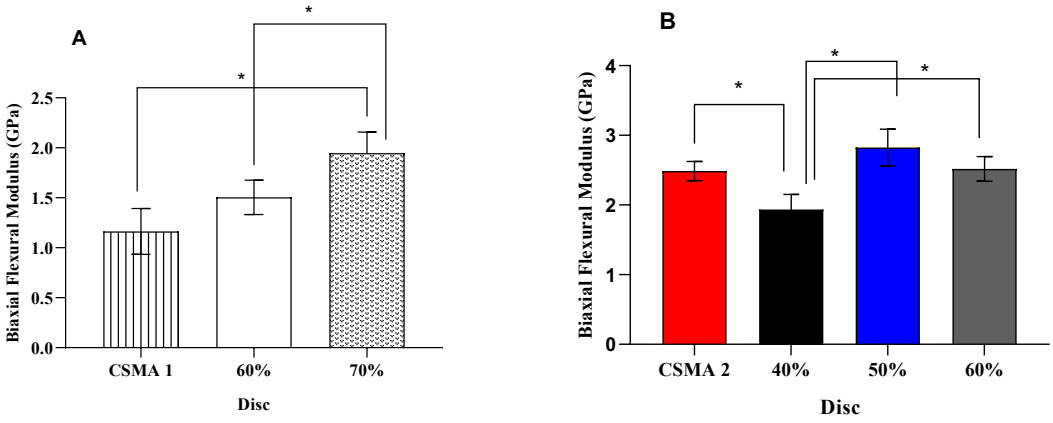

Fig.5. Biaxial Flexural Modulus comparison between CSMA-1 (A) and CSMA-2 (B) polymer formulations ($*p < 0.05$).

It is worth highlighting the benefits of photopolymerisation compared to conventional crosslinking methods in biomedical applications. The use light curable polymers in the field of tissue engineering can allow producing biomaterials in a minimally invasive manner; this involves low energy requirements, fast cure reaction and more importantly solvent free formulations. Moreover, this cost-effective fabrication technique can offer *in situ* material production at room temperature. Consequently, considerable amount of work has recently been dedicated to modification of natural photopolymerisable polymers for regeneration of bone defects in the maxillofacial region.

Zheng et al. (29) developed a degradable scaffold by utilising calcium silicate to simultaneously crosslink silk fibroin and sodium alginate. Although evaluating the compressive stiffness showed an improved mechanical performance, the highest obtained value still remains far from the required modulus in a dynamic environment.

In a similar study, a hydrogel based composite consisting of photocrosslinkable methacrylated glycol chitosan (MeGC) and semi-interpenetrating collagen (Col) was fabricated with a riboflavin photoinitiator under blue light (30). The incorporation of Col in MeGC hydrogels relatively improved the compressive modulus and slowed the degradation rate of the hydrogels. Such findings can provide a useful insight for future research in the field, as sufficient mechanical strength of these scaffolds is still an unmet challenge.

The percentage mass change was calculated with respect to the initial dry weight. The highest degradation rate was observed in 60% CaP composite discs and dropped 10% in weight within the incubation time (**Fig.6**). Slow degradation of this material can provide a more stable environment and prevent sudden pH change upon degradation. This is advantageous in clinical application and can also address the limitations associated with commonly used polymers such as PLGA (11). Incorporation of different amount of CaP fillers and their specific composition are variables that can help us modify various properties of such hybrid systems. Based on the composition of the CaP type of choice in this study, the surface of bioactive MCPM in the hydrated composite can undergo fast dissolution. This will result in the reaction of TCP with the internal MCPM forming brushites, which can eventually induce precipitation of hydroxyapatite minerals to stimulate osteogenesis. The degradation rate of biomaterials is a key factor in determining their potential clinical translation (31) as it needs to match the rate of new tissue formation. Therefore, having a system where degradation can be tailored is highly desired. Short-term degradation of these composites is controlled by the hydrolysis of the powder phase, especially highly reactive MCPM, whereas degradation of the backbone of the liquid phase (CSMA) is a more complex process and requires further investigation. The only clear factor that accounts for degradation of the polymer phase is the degree of crosslinking, which is inversely proportional with the rate

of degradation (32) and can be altered by the percentage of photo initiator of use in the composite paste.

It must be noted that, although the use of TCP can be beneficial due its bone- like mineral phase, it is crucial to find the right balance between the components of the composite to avoid accelerated degradation and volumetric swelling. In a recent study Abert et al. (33) fabricated a scaffold consisting of poly-(D,L-lactide), TCP and calcium carbonate for bone substitutes. Swelling of the polymer matrix was observed due excessive water uptake of the TCP fillers, which can be a concern especially when implanted as a 3D construct with defined dimensions.

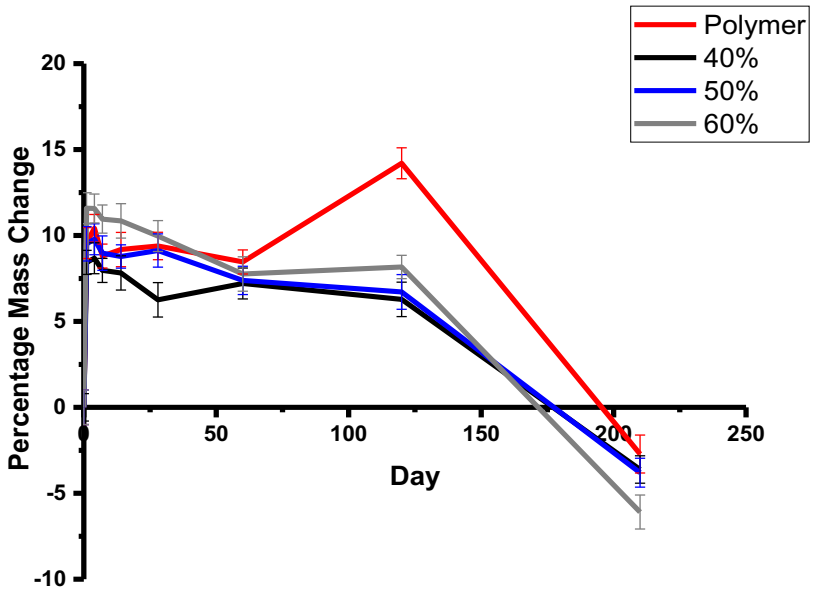

Fig.6. Percentage mass change post 7 months of incubation in distilled water.

The surface hydrophilicity of a biomaterial is crucial to cell adhesion and proliferation (34). Therefore, in order to initially assess the biocompatibility of the discs, the degree of

hydrophilicity was investigated where a glass disc was used as control and all specimens were found to show a hydrophilic behaviour (contact angle<60) (**Fig.7**).

Surface roughness and powder dispersion are the main factors that affect the wettability of the discs. CaP particles increase the surface energy by introducing polar groups into the constructs (OH^- and Ca^{2+}); hence an increase in the powder addition reduces the contact angle. Such changes are explained by Wenzel's equation stating that a large surface area or a rough surface can reduce the contact angle by increasing the polar interaction with water droplets (35). Also, great adhesion between CaP particles and CSMA-2 can account for the observed values where amongst all the composite discs, only 60% was found to exhibit a more significant hydrophilic behaviour (P<0.05).

Acidity of the discs is another critical factor in determining the cytotoxicity of a polymeric system (36). In this study all samples were found to show alkaline behaviour post incubation; the only significant difference was observed between 60% CaP and the control disc, which still remained in the basic range.

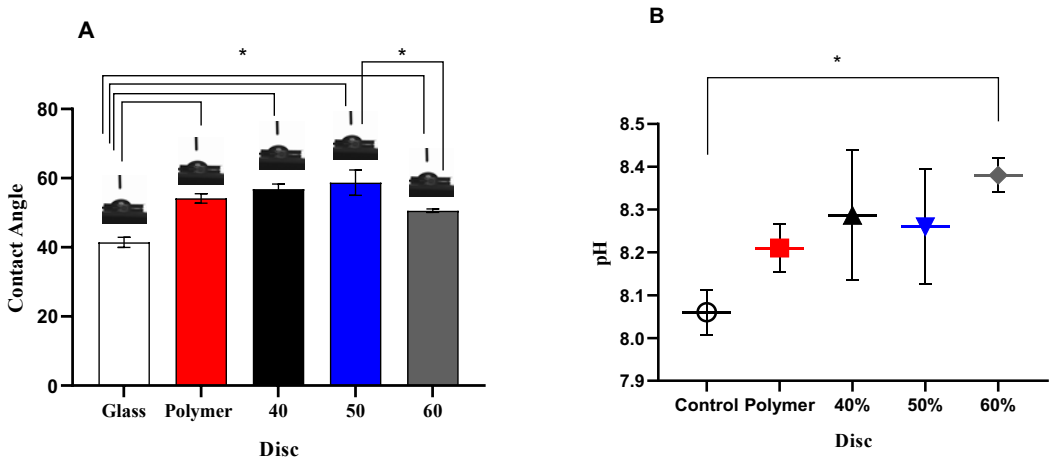

Fig.7. Water contact angle measurements of composite discs compared to a glass control (A) and pH measurements (B) respectively to investigate the acidity of the specimens (*$p < 0.05$)

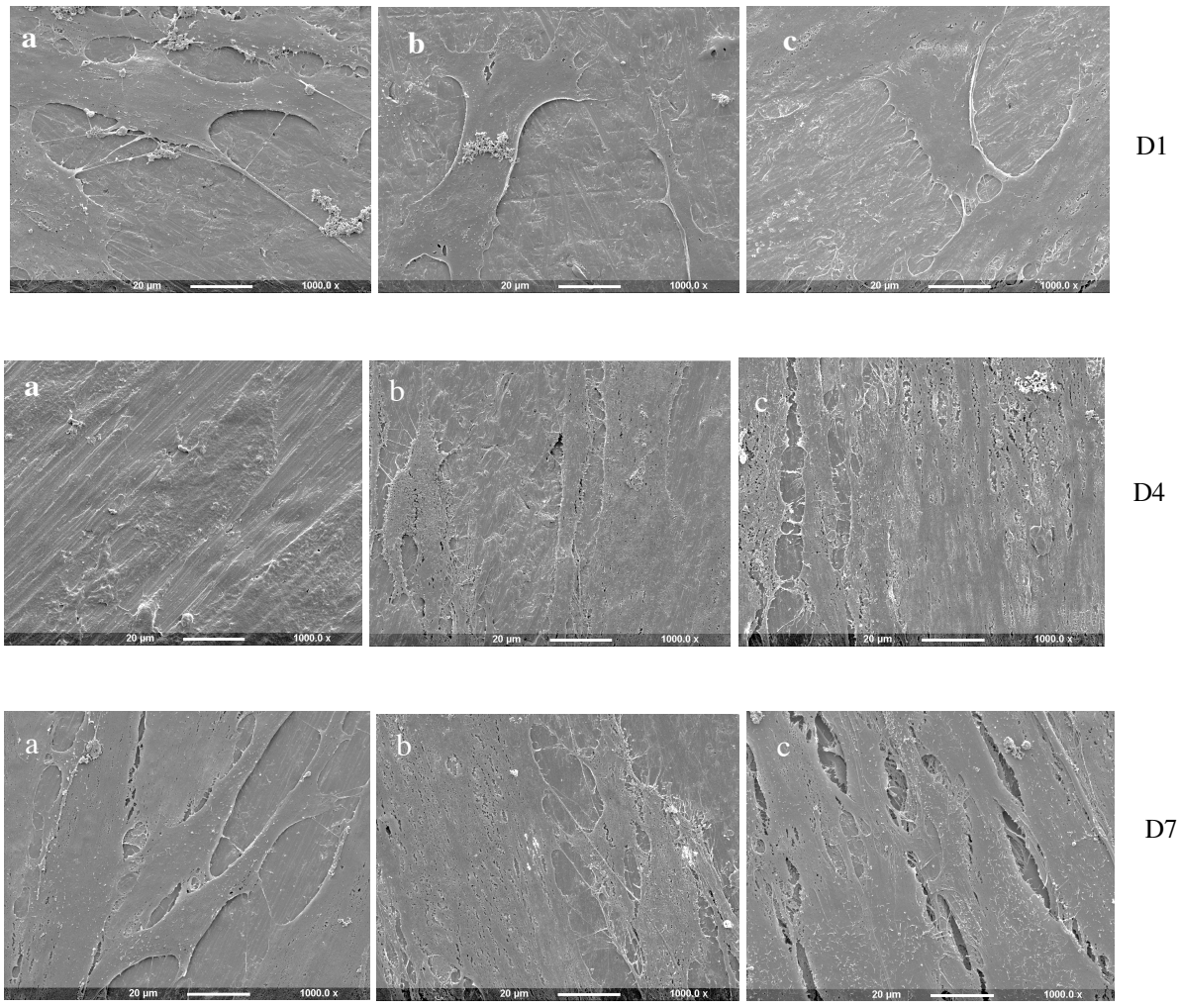

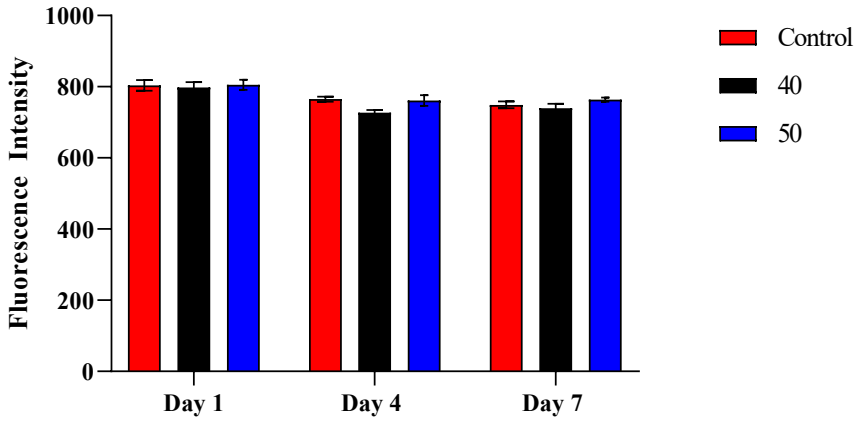

Fig.8. SEM images of control (a), 40%CaP (b) and 50%CaP (c) at day1, 4 and 7 respectively followed by fluorescence intensity measurements showing metabolic activity of the cells on the surface of the discs.

SEM images were taken to investigate the morphology of BMSCs on the surface of the composite discs, 40 and 50, which showed formation of a monolayer of cells on the disc surfaces (**Fig.8**). There was an overall increase in cell processes as well as the alignment and elongation over the incubation period, with no apparent difference in morphological changes in favour of the control group.

Alamar blue assay allowed quantitative measurement of cell metabolism; no significant changes in metabolic activity were observed over the incubation period, this consistent behavior amongst the composite discs and the control can confirm non-cytotoxicity of the specimens (37).

As discussed previously, addition of CaP fillers can play a significant role in biochemical properties of a polymeric matrix. A current *in vitro* study demonstrated that TCP granule scaffolds can improve proliferation of BMSCs and promote the expression of osteogenic

genes and osteogenesis-related proteins (38). Similarly, Feng et al. (39) investigated the effect of addition of Hydroxyapatite (HA) fillers on bioactivity and biocompatibility in a ceramic system. In this study, laser sintering (SLS) technique was used to fabricate the composite scaffolds and HA was incorporated into polyetheretherketone (PEEK)/polyglycolic acid (PGA) hybrid. The results showed that the composite presented a greater degree of cell attachment and proliferation compared to PEEK/PGA scaffolds.

Although CaP powders are known to show improved osteoconductivity and biocompatibility (40), when approaching cell proliferation on the surfaces comprising an organic and inorganic phase, optimum dispersion of the filler into the liquid remains critical. In our study incorporation of 90% TCP and 10% MCPM has helped achieve a more uniform distribution of the powder phase into the polymer (41), which accounts for the observed values (**Fig.8**). Furthermore, future work will be dedicated to surface remineralisation and HA formation on these composite discs which can further enhance the biocompatibility of this system.

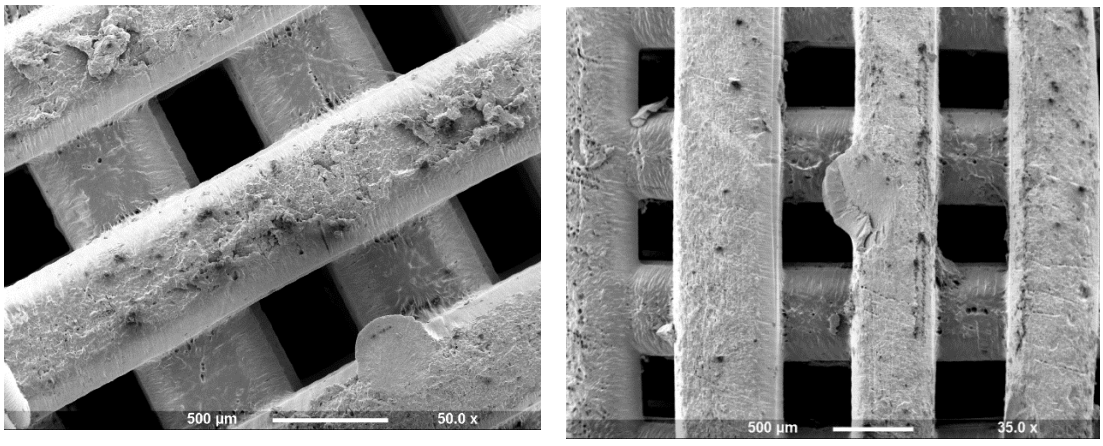

Fig.9. SEM images of 3D printed CSMA-2 at 35x magnification.

3D printing is an emerging technology in the field of tissue engineering. Computer-aided

design and manufacturing (CAD/CAM) processes can offer huge potentials in constructing patient specific implants (42).

In this study the 3D printed CSMA-2 construct (**Fig.9)** was fabricated by the aid of DLP technology. This technique allowed fast curing of the final product and was used in this study as a proof of concept. Utilising this novel technology simply allows manufacturing of a complex system where precise control over the shape and size of the material is provided. Also, this promising technique can provide high resolution printing, which is crucial in bone tissue engineering as it encourages angiogenesis (43). This will address the drawbacks of current techniques by maintaining the internal channel networks of the scaffold necessary for cell proliferation and eventually bone ingrowth(44); it will not require additional surgery to remove the material and finally can be shaped into different configurations to follow the unique contour of craniofacial defects.

CONCLUSION

In this study we successfully synthesised a degradable, low-toxicity and mechanically strong material that can easily be adapted to fit specific needs such as flexibility, stiffness and surface energy by small variations in the manufacturing process. This light curable polymer is targeted at reconstruction of maxillofacial defects, which also has the potential to be used in 3D printing. Future work will be focused on the evaluation of polymer kinetics to provide a better insight into modification of the composite degradation, remineralisation properties and in depth *in vitro* and *in vivo* investigation of this novel system.

Author Contributions

The manuscript was written through contributions of all authors. All authors have given approval to the final version of the manuscript.

REFERENCES

1. Brasileiro BF, de Bragança RMF, Van Sickels JE. An evaluation of patients' knowledge about perioperative information for third molar removal. Journal of Oral and Maxillofacial Surgery. 2012;70(1):12-8.
2. Visser A, Raghoebar GM, van Oort RP, Vissink A. Fate of implant-retained craniofacial prostheses: life span and aftercare. International Journal of Oral & Maxillofacial Implants. 2008;23(1).
3. Lello S, Allen P, Haig S. Aetiology of paediatric facial trauma at a UK District General Hospital. Oral Surgery. 2015;8(4):208-16.
4. UK Cr. Head and neck cancers incidence statistics UK: Cancer research UK; 2017 [Available from: https://www.cancerresearchuk.org/health-professional/cancer-statistics/statistics-by-cancer-type/head-and-neck-cancers/incidence.
5. Steel BJ, Cope MR. A brief history of vascularized free flaps in the oral and maxillofacial region. Journal of Oral and Maxillofacial Surgery. 2015;73(4):786. e1-. e11.
6. Tsuchiya S, Nakatsuka T, Sakuraba M, Kimata Y, Sakurai H, Nakagawa M, et al. Clinical factors associated with postoperative complications and the functional outcome in mandibular reconstruction. Microsurgery. 2013;33(5):337-41.
7. Eppley BL, Pietrzak WS, Blanton MW. Allograft and alloplastic bone substitutes: a review of science and technology for the craniomaxillofacial surgeon. J Craniofac Surg. 2005;16(6):981-9.
8. Lanza R, Langer R, Vacanti JP. Principles of tissue engineering: Academic press; 2011.
9. Xavier JR, Thakur T, Desai P, Jaiswal MK, Sears N, Cosgriff-Hernandez E, et al. Bioactive Nanoengineered Hydrogels for Bone Tissue Engineering: A Growth-Factor-Free Approach. Acs Nano. 2015;9(3):3109-18.
10. Farré-Guasch E, Wolff J, Helder MN, Schulten EA, Forouzanfar T, Klein-Nulend J. Application of additive manufacturing in oral and maxillofacial surgery. Journal of Oral and Maxillofacial Surgery. 2015;73(12):2408-18.
11. Stratton S, Shelke NB, Hoshino K, Rudraiah S, Kumbar SG. Bioactive polymeric scaffolds for tissue engineering. Bioactive Materials. 2016;1(2):93-108.
12. Lin WC, Yao C, Huang TY, Cheng SJ, Tang CM. Long-term in vitro degradation behavior and biocompatibility of polycaprolactone/cobalt-substituted hydroxyapatite composite for bone tissue engineering. Dent Mater. 2019.
13. Cipitria A, Skelton A, Dargaville TR, Dalton PD, Hutmacher DW. Design, fabrication and characterization of PCL electrospun scaffolds-a review. Journal of Materials Chemistry. 2011;21(26):9419-53.
14. Rahim TNAT, Akil HM, Abdullah AM, Mohamad D, Rajion ZA. Mechanical and Morphological Properties of Polyamide 12 Composite for Potential Biomedical Implant: Injection Molding and Desktop 3d Printer. Jurnal Teknologi. 2015;76(7):69-73.
15. Yusa K, Yamamoto O, Iino M, Takano H, Fukuda M, Qiao Z, et al. Eluted zinc ions stimulate osteoblast differentiation and mineralization in human dental pulp stem cells for bone tissue engineering. Archives of Oral Biology. 2016;71:162-9.
16. Garcia JR, Garcia AJ. Biomaterial-mediated strategies targeting vascularization for bone repair. Drug Deliv Transl Res. 2016;6(2):77-95.

17. de Grado GF, Keller L, Idoux-Gillet Y, Wagner Q, Musset AM, Benkirane-Jessel N, et al. Bone substitutes: a review of their characteristics, clinical use, and perspectives for large bone defects management. Journal of Tissue Engineering. 2018;9.
18. Cheng YL, Kao HL. Study on Visible-light-curable Polycarprolactone and Poly(ethylene glycol) diacrylate for LCD-projected Maskless Additive Manufacturing System. Light Manipulating Organic Materials and Devices Ii. 2015;9564.
19. Yang F, Williams CG, Wang DA, Lee H, Manson PN, Elisseeff J. The effect of incorporating RGD adhesive peptide in polyethylene glycol diacrylate hydrogel on osteogenesis of bone marrow stromal cells. Biomaterials. 2005;26(30):5991-8.
20. Liu X, Ma PX. Polymeric scaffolds for bone tissue engineering. Ann Biomed Eng. 2004;32(3):477-86.
21. Bose S, Vahabzadeh S, Bandyopadhyay A. Bone tissue engineering using 3D printing. Materials Today. 2013;16(12):496-504.
22. Zhang AQ, Yang L, Lin YL, Yan LS, Lu HC, Wang LS. Self-healing supramolecular elastomers based on the multi-hydrogen bonding of low-molecular polydimethylsiloxanes: Synthesis and characterization. Journal of Applied Polymer Science. 2013;129(5):2435-42.
23. Lukaszczyk J, Janicki B, Lopez A, Skolucka K, Wojdyla H, Persson C, et al. Novel injectable biomaterials for bone augmentation based on isosorbide dimethacrylic monomers. Mater Sci Eng C Mater Biol Appl. 2014;40:76-84.
24. Johnson AJW, Herschler BA. A review of the mechanical behavior of CaP and CaP/polymer composites for applications in bone replacement and repair. Acta Biomaterialia. 2011;7(1):16-30.
25. Carlsson E, Mestres G, Treerattrakoon K, Lopez A, Ott MK, Larsson S, et al. In Vitro and In Vivo Response to Low-Modulus PMMA-Based Bone Cement. Biomed Research International. 2015.
26. Basha RY, Kumar TSS, Doble M. Design of biocomposite materials for bone tissue regeneration. Materials Science & Engineering C-Materials for Biological Applications. 2015;57:452-63.
27. Ryabenkova Y, Pinnock A, Quadros PA, Goodchild RL, Mobus G, Crawford A, et al. The relationship between particle morphology and rheological properties in injectable nano-hydroxyapatite bone graft substitutes. Materials Science & Engineering C-Materials for Biological Applications. 2017;75:1083-90.
28. Jang JH, Shin S, Kim HJ, Jeong J, Jin HE, Desai MS, et al. Improvement of physical properties of calcium phosphate cement by elastin-like polypeptide supplementation. Scientific Reports. 2018;8.
29. Zheng A, Cao LY, Liu Y, Wu JN, Zeng DL, Hu LW, et al. Biocompatible silk/calcium silicate/sodium alginate composite scaffolds for bone tissue engineering. Carbohydrate Polymers. 2018;199:244-55.
30. Arakawa C, Ng R, Tan S, Kim S, Wu B, Lee M. Photopolymerizable chitosan-collagen hydrogels for bone tissue engineering. J Tissue Eng Regen Med. 2017;11(1):164-74.
31. Chen FM, Liu XH. Advancing biomaterials of human origin for tissue engineering. Progress in Polymer Science. 2016;53:86-168.
32. Niaounakis M. Biopolymers: Reuse, Recycling, and Disposal. Biopolymers: Reuse, Recycling, and Disposal. 2013:1-413.
33. Abert J, Amella A, Weigelt S, Fischer H. Degradation and swelling issues of poly-(d,l-lactide)/beta-tricalcium phosphate/calcium carbonate composites for bone replacement. J Mech Behav Biomed Mater. 2016;54:82-92.
34. Abdallah MN, Tran SD, Abughanam G, Laurenti M, Zuanazzi D, Mezour MA, et al. Biomaterial surface proteomic signature determines interaction with epithelial cells. Acta Biomaterialia. 2017;54:150-63.

35. Carrier O, Bonn D. Contact Angles and the Surface Free Energy of Solids. Droplet Wetting and Evaporation: From Pure to Complex Fluids. 2015:15-23.
36. Alpaslan E, Yazici H, Golshan NH, Ziemer KS, Webster TJ. pH-Dependent Activity of Dextran-Coated Cerium Oxide Nanoparticles on Prohibiting Osteosarcoma Cell Proliferation. Acs Biomaterials Science & Engineering. 2015;1(11):1096-103.
37. Rampersad SN. Multiple Applications of Alamar Blue as an Indicator of Metabolic Function and Cellular Health in Cell Viability Bioassays. Sensors. 2012;12(9):12347-60.
38. Gao P, Zhang H, Liu Y, Fan B, Li X, Xiao X, et al. Beta-tricalcium phosphate granules improve osteogenesis in vitro and establish innovative osteo-regenerators for bone tissue engineering in vivo. Scientific Reports. 2016;6:23367.
39. Feng P, Wei PP, Li PJ, Gao CD, Shuai CJ, Peng SP. Calcium silicate ceramic scaffolds toughened with hydroxyapatite whiskers for bone tissue engineering. Materials Characterization. 2014;97:47-56.
40. Perez RA, Kim HW, Ginebra MP. Polymeric additives to enhance the functional properties of calcium phosphate cements. J Tissue Eng. 2012;3(1):2041731412439555.
41. Abou Neel EA, Salih V, Revell PA, Young AM. Viscoelastic and biological performance of low-modulus, reactive calcium phosphate-filled, degradable, polymeric bone adhesives. Acta Biomater. 2012;8(1):313-20.
42. Yi HG, Choi YJ, Jung JW, Jang J, Song TH, Chae S, et al. Three-dimensional printing of a patient-specific engineered nasal cartilage for augmentative rhinoplasty. J Tissue Eng. 2019;10:2041731418824797.
43. Ma HS, Feng C, Chang J, Wu CT. 3D-printed bioceramic scaffolds: From bone tissue engineering to tumor therapy. Acta Biomaterialia. 2018;79:37-59.
44. Aldaadaa A, Owji N, Knowles J. Three-dimensional Printing in Maxillofacial Surgery: Hype versus Reality. Journal of Tissue Engineering. 2018;9.